

Bimetallic platinum based catalysts for biosensors and energy storage applications

Metini Janyasupab¹, Chen-Wei Liu², Yuan Zhang³, Kuan-Wen Wang², Jiaqiang Xu³, Anna C. Samia⁴, and Chung-Chiun Liu^{1,*}

¹Department of Chemical Engineering, Case Western Reserve University, 2104 Adelbert Road, Cleveland, Ohio 44106-721, USA. ²Institute of Material Sciences and Engineering, National Central University, Chung-Li 320, Taiwan. ³Department of Chemistry, Shanghai University, Shanghai 200444, China. ⁴Department of Chemistry, Case Western Reserve University, Cleveland, Ohio 44106, USA

ABSTRACT

Bimetallic platinum nanoparticles provide great potential in development of catalysts for analytical chemistry and many practical applications. These novel materials offer new properties that are distinct from the pure platinum, and lead to more efficiency in various fuel cell and biosensing systems. In particular, the bimetallic approach has shown electrochemical improvement of platinum catalysts which in turn are limited by poisoning and slow sluggish anodic reaction from both systems. Furthermore, the trends of bimetallic design from theoretical studies and recent experimental results are also discussed for incorporation of the second metals such as Ru, Au, Ni, and Pd. The modified electronic and geometric structures of these metal-pairs with remarkable performances have been comprehensively studied. Therefore, the development of new alloy structures and the systematic study of their properties will have a profound impact for advanced energy and biomedical applications.

KEYWORDS: bimetallic catalyst, platinum catalyst, biosensor, electrochemical detection, fuel cells

CONTENTS

- I. Introduction
- II. Applications and limitations of single Pt metal catalysts in biosensors and fuel cells
 - A. Hydrogen peroxide oxidation
 - B. Methanol oxidation
- III. Bimetallic approach to improve performance of Pt catalysts
- IV. Recent experimental trends in bimetallic catalysts
 - A. Platinum-Ruthenium
 - B. Platinum-Gold
 - C. Platinum-Nickel
 - D. Platinum-other metals
- V. Summary and Outlook

I. INTRODUCTION

Metal catalysts such as platinum (Pt), gold (Au), rhodium (Rh), and palladium (Pd) have been of great scientific and technological interest due to their fascinating optical, electronic, and catalytic properties. The application of these metals in biology, chemistry and engineering disciplines continues to promote major advances in analytical electrochemistry, bioengineering, molecular biology, energy storage materials, and molecular diagnostics. For those applications such as biosensing probes, there are still some important issues in enzyme activity, electron exchange rate, and poor interference capability that

*Corresponding author
cxl9@case.edu

need to be addressed. Due to its excellent conductivity and catalytic properties, metal nanoparticles offer suitable electron transfer enhancement as “electronic wires” between the enzyme redox centers and the electrode surfaces [1]. The introduction of these metal nanoparticles with catalytic properties into biosensors can lower the over potentials of many analytically important electrochemical reactions. For instance, the electroactivity of laccase in the detection of catechins was promoted by dendrimer-encapsulated Au nanoparticles (AuNPs) [2]. The quasi-reversible redox peak of the Cu redox center of the laccase molecule was observed at $-0.03/+0.13$ V vs Ag/AgCl, and the electron-transfer rate constant was determined to be 1.28 s^{-1} . Moreover, based on the selective catalytic activity of metal nanoparticles, selective electrochemical analysis could be also improved. For example, a novel assembled nanobiosensor constructed with the combination of Cd Te quantum dots and Au nanoparticles was designed for the direct determination of glucose in serum with high sensitivity and selectivity [3]. Additionally, Ir nanoparticle catalysts were incorporated in the carbon-based working and counter electrodes, which resulted in the enhancement of the performance of the biosensor for fructosylvaline detection [4].

Recently, there has been an increasing trend of research interest in developing more efficient electrocatalysts. In particular, development of bimetallic catalysts by using nanoscience and nanotechnology is one of promising approaches to design new materials. Because of their synergistic effect, the bimetallic catalysts such as random alloys, intermetallic alloys, and core/shell particles can provide not only different structures, but also a diverse range of elemental compositions, leading to an improvement in electrocatalytic performance. In this article, we will review the basics of the single Pt system, and the rationale that leads to the bimetallic design approach in order to demonstrate the increasing trend of bimetallic catalysts for analytical electrochemistry and for practical applications in biosensors and fuel cells.

II. Applications and limitations of single Pt metal catalysts in biosensors and fuel cells

Pt has been extensively used as a catalyst. In the C-H activation reaction, efficient, selective, and

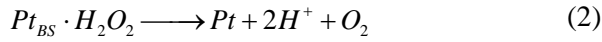
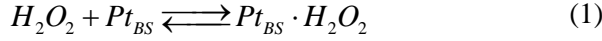
direct functionalization of hydrocarbons can be carried out by Pt complexes [5]. Pt also plays a crucial role in the abatement of environmental pollution in automotive and industrial exhausts. They are implemented for converting nitrogen oxides (NO_x), carbon monoxide, sulphur oxide (SO_x), and many different organic compounds into less harmful species [3, 4, 6]. In addition, Pt is often integrated in electrochemical sensors and biosensors [7-9] as a catalyst that provides many practical applications directly related to analytical chemistry. Consequently, understanding the role of Pt catalyst in the reaction mechanisms of these systems is worthwhile to design suitable electrochemical and biosensing platforms.

Different shapes of Pt can provide different surface controlled structure. For instance, not only do cubic-like particles exhibit large (100) facets but also (111) and (110) facets [9]. Truncated tetrahedral particles prepared by the shape controlling technique exhibit only (111) and (100) facets [9]. Similarly, octahedron-like Pt particles have both (111) and (100) facets, but the area ratio of (100) to (111) varies depending on the relative growth rate of the two surfaces [9]. This is important to determine the catalytic activity because certain facets such as (110) are believed to be the high surface energy facets. In addition, it has also been mentioned that Pt might not be stable over prolonged periods of time due to chemical dissolution or chemisorbed species in the electrolyte [10]. Therefore, studies of catalytic mechanisms in the Pt system are necessary to understand the behavior of Pt metal in both biosensor and fuel cell systems for practical application purposes. Here, we demonstrate two most commonly used catalytic reactions of (A) hydrogen peroxide oxidation in biosensors, and (B) methanol oxidation in direct methanol fuel cells (DMFC) using single Pt catalysts.

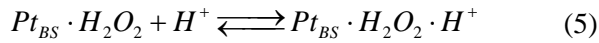
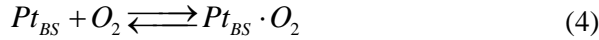
A. Hydrogen peroxide oxidation

The mechanism of H₂O₂ (a main by-product of many human enzymatic reactions) oxidation using Pt catalysts has been investigated. A series of studies by Hall *et al.* have reported the formation of chemisorbed species coming from the reaction products (O₂ and/or H⁺) on the surface of Pt catalysts [11]. The mechanism of H₂O₂ oxidation by Pt involves a binding interaction of H₂O₂ to active surface sites, forming a surface complex as

indicated in Eq. 1. Then, $Pt_{BS} \cdot H_2O_2$ undergoes an internal charge transfer that results in the reduction of the binding site (Eq. 2), which is then electrochemically oxidized to reform active binding site Pt_{BS} as shown in Eq. 3.



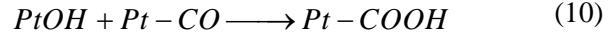
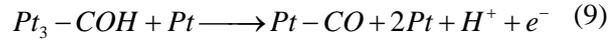
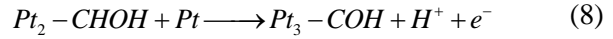
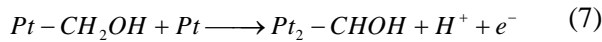
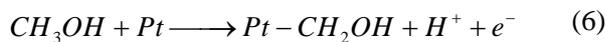
However, there are two competitive mechanisms that inhibit the hydrogen oxidation reaction above. The intermediate species (i.e. O_2 and H^+) shown in Eq. 4-5 is also easily adsorbed on the Pt active sites, thereby resulting in the poisoning of the Pt catalysts.



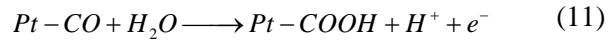
Related to electrochemical analytical chemistry and biosensor applications, a low catalytic performance needs relatively more external power to operate. As a result, the single Pt nanoparticles require a relatively higher applied potential when used for the detection of H_2O_2 compared to bimetallic nanoparticles [12]. Thus, at higher applied potential, interference contributed by many co-existing species in the solution could be oxidized. This leads to poor selectivity of the single Pt metal catalyst in quantifying H_2O_2 .

B. Methanol oxidation

Similar to H_2O_2 oxidation process, Pt is also used for the oxidation of methanol and ethanol in low-temperature fuel cell applications [13, 14]. Its superior catalytic activity, however, drops dramatically with time when carbon monoxide poisoning becomes apparent. In the case of the methanol oxidation reaction (MOR), the mechanism can be summarized in terms of two basic processes [15]: (a) electrosorption of methanol onto the catalysts; and (b) addition of oxygen to adsorbed carbon-containing intermediates to generate CO_2 as illustrated in Eq. 6-12.



or



Methanol can be oxidized to CO_2 via a CO or $HCOO^-$ reactive intermediates and the formation of strongly adsorbed linearly bonded CO leads to the self-poisoning of Pt electrocatalysts. The poisoning of the catalysts significantly decreases the activity of Pt catalysts resulting in poor durability. Furthermore, at potentials above +0.6 V vs RHE, the corrosion of Pt nanoparticles yields formation of Pt^{2+} ionic species and pronounced undesirable Pt element redistribution at the cathode. These problems necessitates the need to employ a bimetallic system approach, whereby a second metal is alloyed to Pt in order to control the equilibrium geometry, modify the electronic structure and the binding energy of the Pt catalysts in order to resolve the catalyst's deterioration issues [16].

III. Bimetallic approach to improve performance of Pt catalysts

A rationale to utilize bimetallic catalysts was established from the so-called *volcano plot*, which describes a relationship of the catalytic activity in terms of energy between adsorbate and metals. Fig. 1 shows the volcano plot of single metallic catalysts in the oxygen reduction reaction in fuel cells. The metals (e.g. Au, Ag) towards the right of the volcano plot indicate stronger bonding to oxygen, which encounters larger activation energy for O_2 dissociation. In contrast, the interaction of the formed metal oxide towards the left of the plot is too strong to release O or OH species, which in turn subsequently reduces the coverage of available active sites on the metal surface. Therefore, the optimal catalytic activity is often found in the middle where moderate energy requirements can both minimize problems associated with the O_2 dissociation and O /OH removal processes.

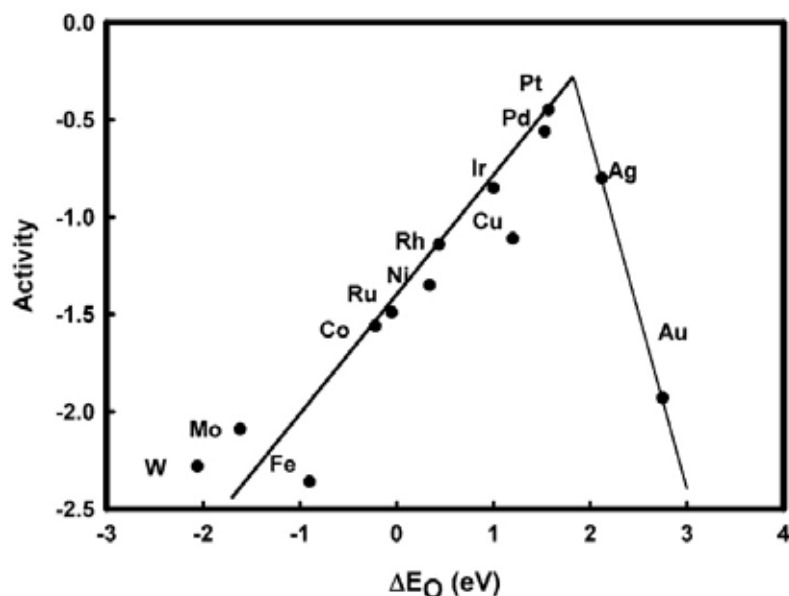


Fig. 1. Trends in oxygen reduction activity plotted as a function of the oxygen binding energy. Reprinted with permission from Norskov, J. K. *et al.*, *J. Phys. Chem. B*, 108, 17886. Copyright [2004], American Chemical Society.

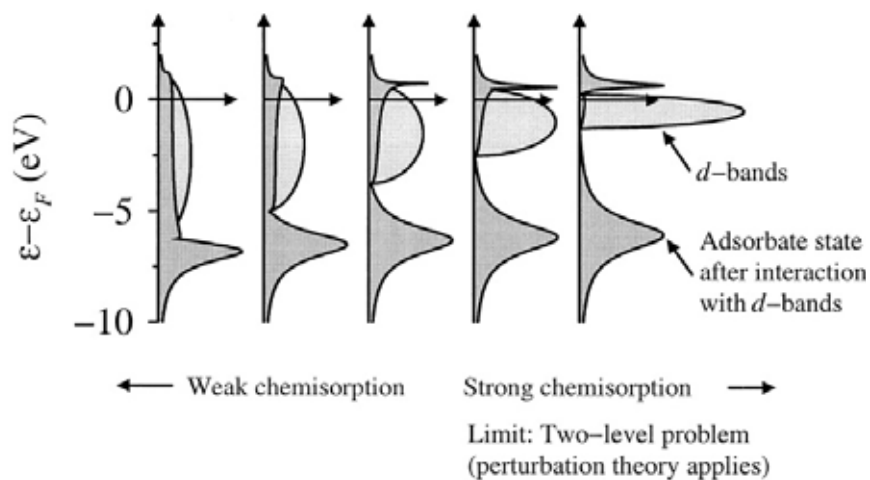


Fig. 2. The local density of states projected onto an adsorbate state interacting with the d-bands at a surface. As d-band width decreases, the d-band center is shifted up and the anti-bonding state is emptied above the Fermi level and the bond becomes stronger. Reprinted from Hammer, B. *et al.*, *Adv. Catal.*, Academic Press, 71, Copyright (2000) with permission from Elsevier.

Although the single Pt, Pd, or Rh metal is highly active towards the oxygen reduction reaction, it has poor selectivity due to self-poisoning [17]. Because many other intermediate species, e.g. CO, require less energy than the oxygen molecule to form an interaction with the metal, the competition to occupy available active sites on

metal surface occurs. Consequently, the metal oxide coverage substantially decreases and thus become less accessible to oxygen. In addition, incomplete cycle of catalysis increases due to an irreversible process of metal-CO formation. Therefore, the approach of alloying metals involves the intrinsic tuning of electronic or modification

of the geometric structure of the catalysts at atomic level. For a proper modification of electronic structure, most of the transition metals interact with the adsorbate in d-band. Based on the tight bonding theory, the occupancy of localized electrons in d-band structure varies along different metals as they shift through the Fermi level [18]. As shown in Fig. 2, the broader the width of d-band in the metal surface (light grey) the lower the d-band center (ϵ_d) is shifted downward away from the Fermi level, and vice versa. As a result, a number of bonding state increases (become filled), and the bond strength to the adsorbate decreases. Based on this atomic-adsorbate interaction, the density functional theory (DFT) can be applied to calculate the chemisorptive bonds in order to predict behavior of bimetallic catalysts.

Because the chemisorption energy profoundly affects the surface activity, Hammer and Norskov [20] suggested many possible factors to alter the electronic and geometric structure of metals. Strain and ligand effects, corresponding to metal-adsorbate and metal-metal interactions, respectively, are most widely discussed in the literature [19]. In Fig. 3, Greeley *et al.* illustrated theoretical trend in bimetallic Pt-based catalysts calculated by the DFT model, which is related to d-band center for oxygen reduction reaction in fuel cells. In this work, the formation of Pt-skin in the Pt₃M catalyst system would modify electronic structure, exhibiting a better catalytic activity than the single Pt by roughly tuning the stability of the oxygen adsorbate.

Similar work by Stamenkovic [21] also demonstrates a relationship between oxygen adsorption energy and the d-band centers of Pt₃Ti, Pt₃Fe, Pt₃Co, Pt₃Ni and single Pt for O₂ dissociation in Fig. 4(a). As discussed earlier, O and OH removal becomes a rate determining step and causes a loss of activity in the single Pt metal catalyst. Based on DFT analysis, the d-band center is calculated from the density of the state resulting from the oxygen-metal bonding (Fig. 4b). The oxygen adsorption energy tends to increase as the d-band center shifts more negatively. As a result, weaker interaction between metal and surface oxide formation in the case of Pt₃Ni exhibits significantly higher catalytic activity as compared to the single Pt in Fig. 4(c). However, too much downward shift of d-band center (e.g. in the case of Pt₃Ti)

encounter too large energy barrier to break O₂ bond, thereby exhibiting less activity. Thus, for an optimum performance design, the catalyst needs to compromise both the O₂ dissociation process and critical intermediates (e.g. O, OH) formation on the metal surface.

IV. Recent experimental trends in bimetallic catalysts

As described by theoretical rationale, bimetallics provide a promising approach to modify catalytic properties. Shown by several experimental studies, the following section includes the most commonly used Pt-based bimetallic catalysts with Ru, Au, Ni and other metals in fuel cell and biosensor systems. Recent trends of design will also be discussed to demonstrate the use of incorporating these alloyed metals into the electrochemical system as well as illustrate the analytical results of their enhancement in catalytic performance.

A. Platinum-Ruthenium catalysts (Pt-Ru)

Bimetallic Pt-Ru catalyst is one of the early metal-pair investigated for enhancing the catalytic activity of Pt in the hydrogen oxidation reaction (HOR). As mentioned earlier, the single Pt metal surface is difficult to dissociate with CO_{ads} on the anode. As a result, the Pt-CO is likely to occupy the Pt active sites, leading to surface poisoning. In spite of a small CO amount (5-20 ppm) in the H₂ streamline [22], it is inevitable to prevent the poisoning effect on Pt metal. Papageorgopoulos and de Bruijn [23] showed that with only 1% CO/hydrogen mixture, CO blocks 98% of the active site at 25°C. The study also found that CO_{ads} can be removed from the Pt active sites by increasing the anodic potential to 0.7 V to form CO₂. However, operating fuel cell at this high potential would be impractical and cause a serious loss of efficiency.

In 1987, an early investigation by Watanabe and Motto [24] demonstrated that the electro-oxidation activity of a PtRu catalyst in the H₂ streamline is higher than that of the pure Pt metal. It was believed that Pt-Ru follows the so-called bi-functional mechanism to alleviate poisoning by migrating CO to Ru. As shown in Fig. 5, Ianniello demonstrated that the CO oxidation in Pt-Ru alloy occurs at 170-200 mV, lower than that of pure Pt [25].

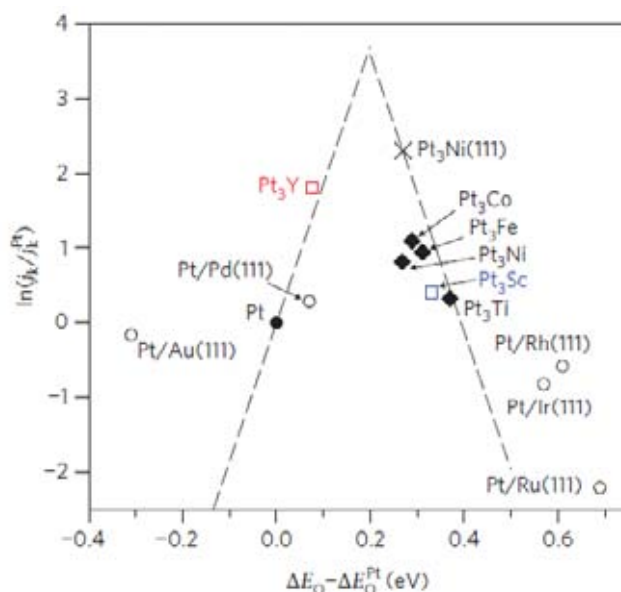


Fig. 3. Volcano plots and free-energy diagrams for the oxygen reduction reaction on Pt-based transition metal alloys. Measured kinetic current density as reported in the literature for a range of alloy electrocatalysts with Pt ‘skins’ plotted as a function of the calculated oxygen adsorption energy. The sources of the experimental data are marked by: circles (Pt monolayers supported on single-crystal metal electrodes), diamonds (polycrystalline alloys annealed in ultrahigh vacuum before immersion in the electrochemical cell) and crosses (bulk Pt₃Ni (111) alloys annealed in ultrahigh vacuum before immersion). The dashed lines are the theoretical predictions. The Pt₃Y (red) and Pt₃Sc (blue) catalysts were studied in the ref. [20]. Reprinted by permission from Macmillan Publishers Ltd: Nat. Chem., Greeley, J. *et al.*, 1, 552, copyright (2009).

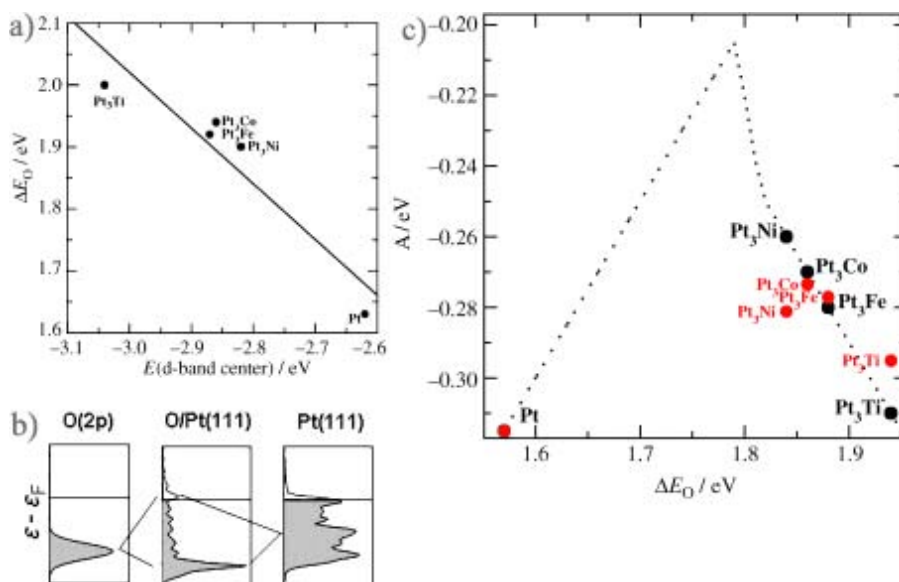


Fig. 4. (a) The correlation between the d-band center and the oxygen adsorption energy calculated by DFT; (b) from left to right, sp-broadened 2p orbital for O(g), projected p density of states of oxygen atoms on Pt(111), and projected d density of states of Pt(111); (c) Activity versus the experimentally measured d-band center relative to Pt. The activity predicted from DFT simulations is shown in black, and the measured activity is shown in red. Reprinted from Stamenkovic, V. *et al.*, 2006, Angew. Chem. Int. Edit., 45, 2897., with permission from John Wiley and Sons.

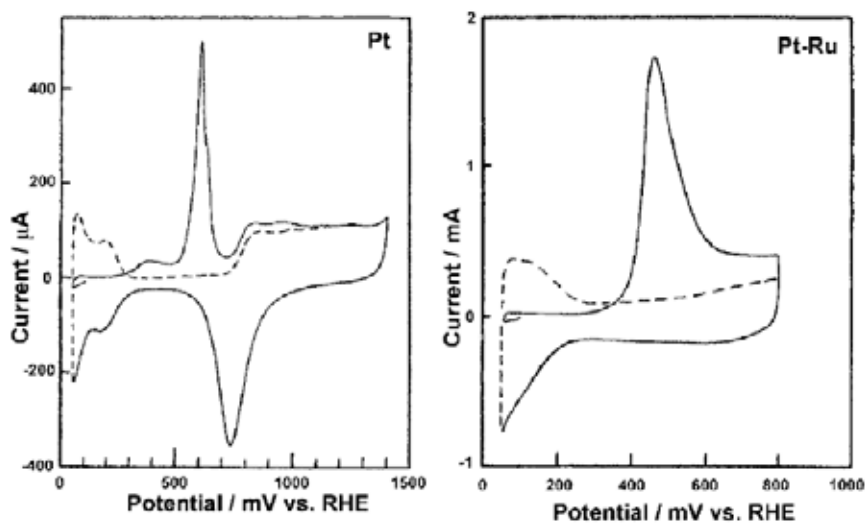


Fig. 5. Comparison of the oxidation of CO on Pt and Pt-Ru. Reprinted from Ianniello, R. *et al.*, *Electrochim. Acta*, 39, 1863, Copyright (1994) with permission from Elsevier.

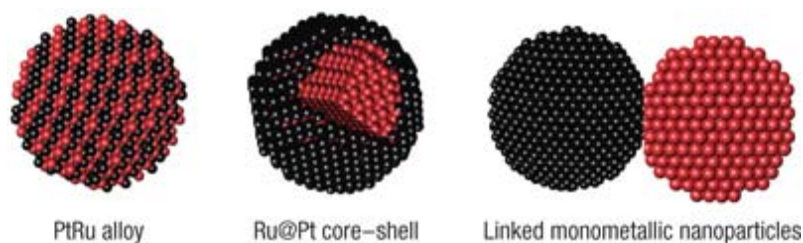


Fig. 6. Graphical representation of alloy, core-shell and linked monometallic nanoparticles in the Pt-Ru bimetallic system. Reprinted by permission from Macmillan Publishers Ltd: *Nat. Mater.*, Alayoglu, S. *et al.*, 7, 333, copyright (2008).

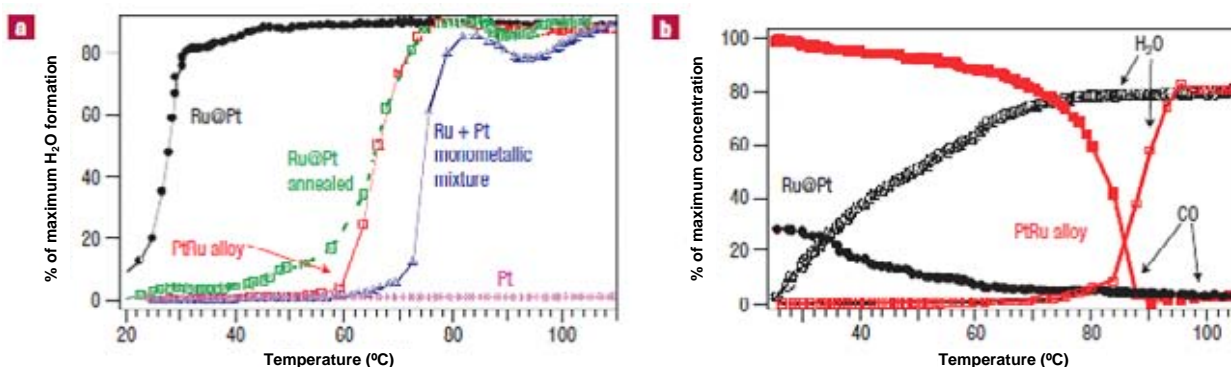


Fig. 7. Catalytic results for core-shell and alloy PtRu particles. a) H_2O formation versus temperature for H_2 feeds contaminated by 0.1% CO by volume. b) % formation of H_2O (open symbols) and % CO conversion (filled symbols) plotted against temperature for the core-shell (black) and alloy (red) nanoparticles catalysts for H_2 feeds contaminated by 0.2% CO. Reprinted by permission from Macmillan Publishers Ltd: *Nat. Mater.*, Alayoglu, S. *et al.*, 7, 333, copyright (2008).

Moreover, unlike the pure Pt, the bimetallic Pt-Ru has a different electronic structure, which results to lower potential for dissociation of water. Due to the lower activation energy of oxygen adsorption, water is preferentially adsorbed on the Ru sites and subsequently forms Ru-OH. This allows CO_{ads} on the Pt sites to oxidize at the adjacent Ru-OH, thereby removing the poison on the Pt sites [26]. Furthermore, another possible contribution of alloying in Pt-Ru is believed to be the weakening of the Pt-CO bonding, which would in turn facilitate the formation of CO_2 [23, 27, 28]. As a result, the electronic structure of the alloy is altered and contributed to improved HOR efficiency.

In an agreement to its HOR activity, the PtRu performance in DMFC exhibits similar trends in improvement as demonstrated in several studies [21, 29-35]. Not only does DMFCs encounter slow anodic reactions from breaking C-C bonds, the cathode performance is also degraded by methanol crossover [36-38]. Driven by concentration gradient, methanol diffuses across the membrane from the anode to the cathode side. Consequently, the oxygen reduction reaction on the cathode decreases. Especially at low temperature (30°C), methanol crossover is strongly pronounced at the cathode through the Nafion membrane [39]. In the last five years, controllable and surface design of Pt-Ru catalysts demonstrated improvement in catalytic performance.

Recently, trends in structural designs and surface science techniques have been integrated to enhance the analytical performance of bimetallic catalysts. Alayoglu and co-workers [40] have shown that a Pt monolayer on metal based alloy, also known as near-surface alloy (NSA), (right structure in Fig. 6), exhibit an improvement in HOR activity [41, 42]. Similar work by this research group has also shown another structural design of Ru core@Pt-shell (middle structure in Fig. 6) to show a uniform architecture. Unlike NSA, the core-shell structure only reveals one type of atom (Pt) on the surface and demonstrates both ligand and strain effects of bi-functional mechanism. Fig. 7 emphasizes a remarkable performance of the core-shell Pt-Ru design in CO oxidation at low temperature (30°C) in HOR, exhibiting significantly superior to traditional Pt-Ru alloy (85°C), NSA (93°C), and single Pt (170°C). Although this opens up a new possibility to design more active and more selective alloys, the role of unexposed Ru core and Pt shell to modify electronic structure is beyond bi-functionality and not fully developed. In addition to structural modification, introducing a third and/or more metals has also shown some improvements. Park and co-workers [43] reported the effect of incorporating tungsten oxide WO_3 into the PtRu system that exhibited a superior MOR activity compared to PtRu and Pt (Fig. 8). Following similar trends, tungsten [43-45],

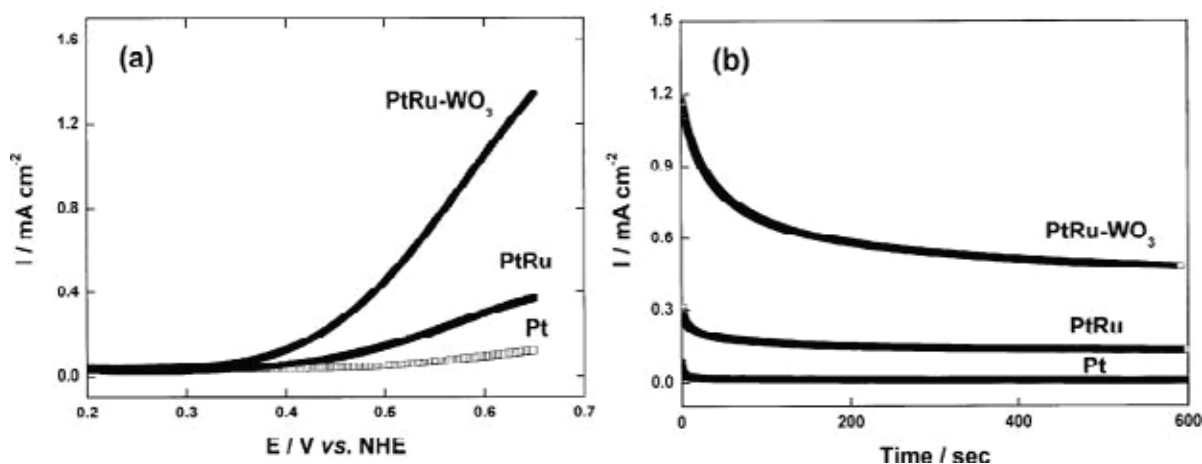


Fig. 8. (a) Current density vs accelerating potentials for the PtRu- WO_3 nanostructured electrode, PtRu, and Pt thin-film electrode and (b) plot of current density vs time at the oxidation potential of +0.6 V. Reprinted with permission from Park, K. W. *et al.*, Appl. Phys. Lett., 82, 1090, Copyright [2003], American Institute of Physics.

molybdenum [46-48], cobalt [49, 50], tin [48, 51, 52] and nickel [48, 50, 53] have gained interest in improving the Pt-Ru system by further tuning more favorable surface oxide properties, in order to optimize CO tolerance and catalyst stability.

As proven with many fuel cell catalyst systems, Pt-Ru catalysts can be applied to biosensing applications with the same objective of improving

the analytical quantification process. The contributions of this bimetal in this field include: (i) enhancement of selectivity from intermediate species in blood, serum, or physiological fluids, (ii) lowering of the applied potential in operation, or (iii) facilitation of catalytic activity due to a better interaction to target species. Recent work in our research group [54] has shown that Pt-Ru catalysts have higher

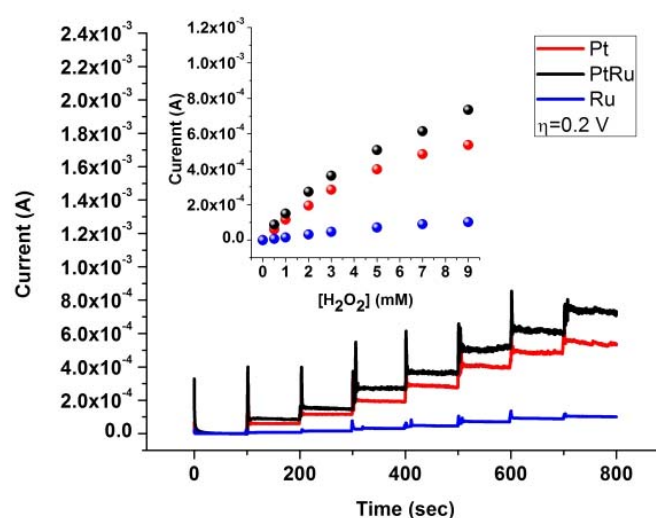


Fig. 9. Amperometric measurements (left) in H₂O₂ detection at overpotential of +0.2 V on single Pt, Pt-Ru and single Ru catalysts. Reprinted from [54] with permission.

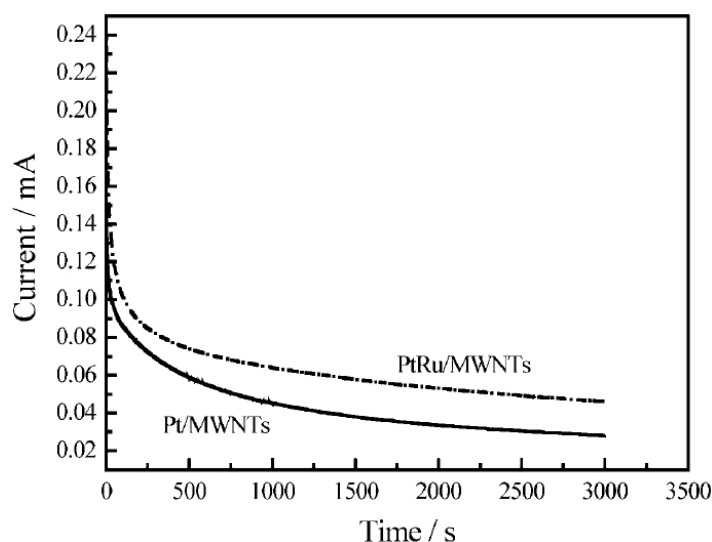


Fig. 10. Chronoamperometric response of 25.0 mM glucose in NaOH at +0.55 V applied potential on Pt and Pt-Ru with multi-wall carbon nanotube. Reprinted from Li, L. H. *et al.*, 2008, *Electroanalysis*, 20, 2212, with permission from John Wiley and Sons.

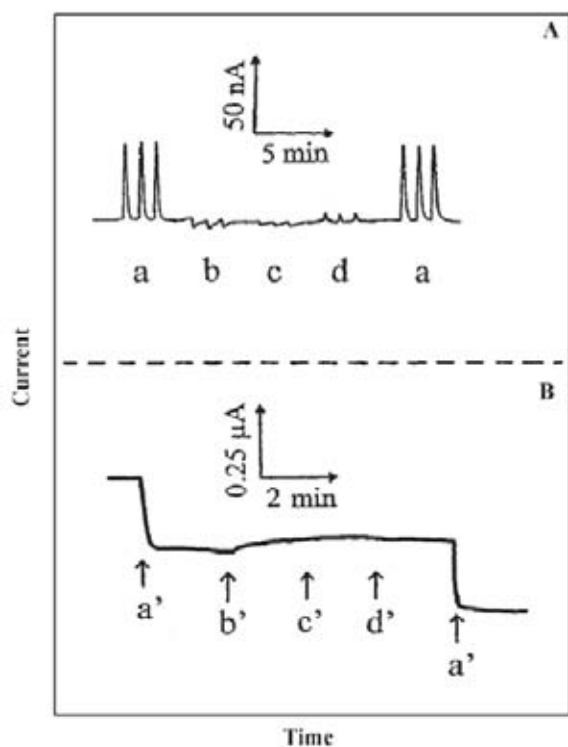


Fig. 11. Flow-injection (A) and batch (B) amperometric signals at the Pt-Ru-dispersed carbon paste glucose oxidase electrode for addition of 8 mM glucose (a); 0.4 mM ascorbic acid (b); 0.4 mM uric acid (c); 0.4 mM acetaminophen (d); 5 mM glucose (a'); 0.1 mM ascorbic acid (b'); 0.1 mM uric acid (c'); and 0.1 mM acetaminophen (d') [57].

sensitivity towards H_2O_2 detection, which is about 30% improvement compared to single Pt (Fig. 9). The Pt-Ru catalysts utilized in our group were prepared via a borohydride reduction process of metal salts in aqueous solutions. Using a different microwave assisted synthesis approach that utilizes ethylene glycol, Pt-Ru catalysts were shown to exhibit almost twice higher sensitivity than the single Pt metal [55]. Furthermore, Li *et al.* [56] demonstrated a higher steady state kinetic current in glucose oxidation with Pt-Ru as compared to the use of Pt on multiwalled-carbon nanotubes (Fig. 10). Jie Liu and Joseph Wang [57] reported an enhancement in using PtRu catalysts to selectively oxidize glucose in the presence of interfering species such as ascorbic acid, uric acid, and acetaminophen for both flow injection and stationary detection as shown in Fig. 11. Currently, PtRu has successfully demonstrated

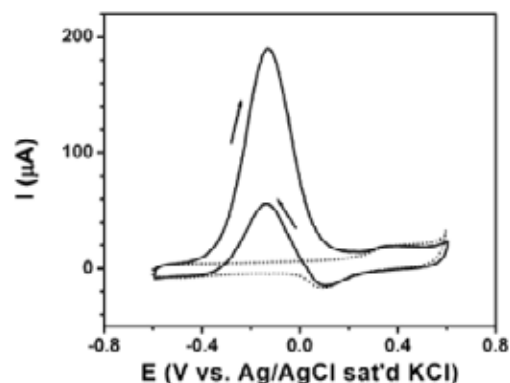


Fig. 12. CV curves for a 24% $\text{Au}_{81}\text{Pt}_{19}/\text{C}$ catalyst in 0.5 MKOH electrolyte with (solid curves) and without (dash curves) 0.5 M methanol. Scan rate: 50 mV/s. Reprinted from Luo, J. *et al.*, Catal. Today, 99, 291, Copyright (2005) with permission from Elsevier.

evidence of improvement to quantify analytes in biological samples. In spite of the few studies previously mentioned in using PtRu, further development on both structural and elemental designs can offer a new biosensing platform to extend more capability in medical diagnosis.

B. Platinum gold catalysts (Pt-Au)

Among the different Pt-based catalysts, the Pt–Au alloy system has been recognized as the recent most popular catalysts in the field of fuel cell and biosensor applications. Numerous studies have shown that the addition of Au can have a synergistic catalytic effect for various fuel cell reactions such as the methanol oxidation reaction (MOR) and the oxygen reduction reaction (ORR) [58–68]. For MOR, the Pt-Au alloy catalysts offer a bi-functional mechanism or an electronic effect in which the surface of Pt provides the main site for the dehydrogenation and the use of Au helps to modify the surface adsorption/desorption properties for reactants, intermediates, or products, which can help to both modify the electronic structure of surface adsorption and restrain adsorbed poisonous species such as CO. Fig. 12 presents CV curves obtained for methanol oxidation at $\text{Au}_{81}\text{Pt}_{19}/\text{C}$ catalysts in electrolyte [58]. A typical methanol oxidation peak is observed at the same potential for the $\text{Au}_{81}\text{Pt}_{19}/\text{C}$ catalyst.

For instance, Choi *et al.* [69] have reported that less amount of CO is adsorbed on the surface of

PtAu catalysts after oxidizing more methanol compared to pure Pt. It was found that the PtAu alloy catalysts may exhibit an alternative route for methanol oxidation by avoiding the formation of adsorbed CO, which is different from the PtRu catalytic system. The electrocatalytic activity of PtAu catalyst for MOR has shown a lower onset potential and a larger current density than pure Pt. On the other hand, for PtAu bulk alloy catalysts used in alkaline electrolytes in addition to the decrease in activation energy for facilitating oxidative desorption and suppressing the adsorption of CO, the use of Au may play an important role in reducing the strength of the Pt-OH formation [58]. In addition, a strong adsorption of CO on surface Pt sites due to the presence of surface Au, as predicted by density functional theory (DFT), may cause the deterioration of the electroactivity [70]. Furthermore, Du *et al.* [71] demonstrated a coverage-related study of Pt deposited onto Au surface. The continuous atoms of Pt on the surface are needed for enhancing methanol dehydrogenation on Pt sites and could weaken the adsorption strength of CO_{ads} .

On the other hand, based on the thermodynamics principle, the possible assumption is also proposed for designing bimetallic catalysts. This suggestion implies that one metal in the alloy breaks the O_2 bond and the other one acts to reduce the resulting adsorbed O [72]. Furthermore, Stamenkovic *et al.* [73] have proposed a trend to develop better catalysts than Pt for ORR. The catalyst should counterbalance two opposing effects, a comparatively strong adsorption energy of O_2 and a comparatively low coverage by oxygenated species in order to design better catalyst for ORR. Hence, a synergistic effect for Pt–Au alloy catalysts was suggested by a higher lying d-band center of Pt for O_2 bond breaking and a lower one for Au - OH bond formation. For example, Hernandez-Fernandez *et al.* [67] claimed that the adsorption energy of O_2 for various of transition metals generally augments with the vacancy in the d-orbital valance. Therefore, the oxophilicity of the Pt electrode has been modified by alloying with Au, exhibiting the remarkable performance for ORR [74]. The promotional effect for Pt-Au electrodes are attributed to a decrease in d-orbital vacancy of Pt by alloying with Au and

modification of the Pt-Pt interatomic distances. Liu *et al.* [75] investigated alloy catalysts of PtAu/Ce_xC with various Ce additions (x) for the ORR. Their data demonstrated that when compared to commercial Pt/C catalysts, a significant enhancement of onset potential for ORR were noted for PtAu/Ce_xC (x = 10-20) catalysts. This promotion may be attributed to not only the modification of the oxophilicity of PtAu/Ce_xC catalysts and enhancement of the removal rate of surface oxide, but also improvement in the dispersion of d_{PtAu} and the segregation of Pt. Bus *et al.* [76] demonstrated that based on X-ray absorption near-edge spectroscopy (XANES) studies, the electronic structure of Pt and Au clusters differs from that of the corresponding monometallic clusters due to the alloying and distance effects, followed by interatomic charge restructuring for the Au 5d and Pt 5d bands. Moreover, as predicted from DFT, the pure Pt(111) and Pt/Au(111) supported with Pt monolayer on the top have shown significant improvement for ORR activity [77, 78]. On the other hand, Pt nanoparticles modified by Au clusters displayed highly stable activity after 30,000 potential cycles between 0.7 and 1.1 V. The durability for the Pt-Au catalysts was attributed to the stabilization effect of the Au clusters, suppressing Pt dissolution during ORR [79]. Fig. 13 shows the ORR curves for Au/Pt/C (A) and Pt/C (C) catalysts before and after 30,000 potential at a rotation rate of 1600 rpm. The electrocatalytic activity of Au/Pt/C for ORR, obtained before and after 30,000 potential cycling, showed a smaller degradation in potential region (Fig. 13A) than that of Pt/C, which exhibited significant degradation over the potential region (Fig. 13C). By measuring the surface-area of Au/Pt/C and Pt/C, it can be seen that there is no change for both catalysts before and after 30,000 potential cycling (Fig. 13B). However, for Pt/C, the huge loss of Pt surface area is observed after potential cycling (Fig. 13D) [79].

In addition, the bimetallic Pt-Au catalysts have also been used in biosensor applications and were found to exhibit higher electro-catalytic activities toward hydrogen peroxide (H_2O_2) oxidation than Pt alone. In the work of Singh *et al.* the PtAu/C nanocomposites with Pt:Au (1:3) have shown

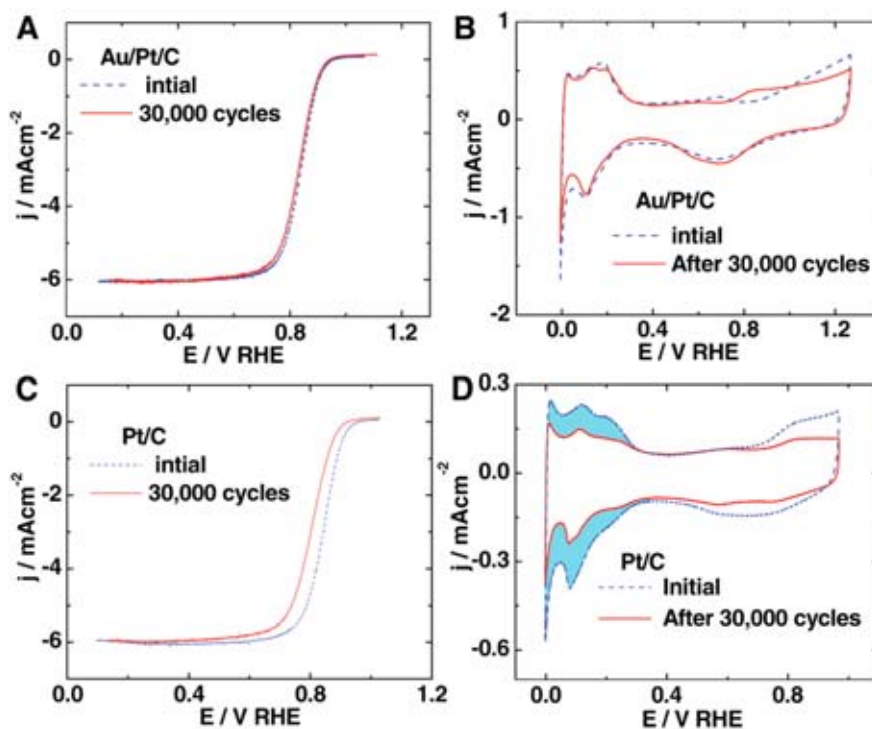


Fig. 13. ORR curves for Au/Pt/C (A) and Pt/C (C) catalysts on a RDE, before and after 30,000 potential cycles at a sweep rate of 10 mV/s with a rotation rate of 1600 rpm. CV curves for Au/Pt/C (B) and Pt/C (D) catalysts, before and after 30,000 cycles at sweep rate of 50 and 20 mV/s, respectively. From Zhang, J. *et al.*, 2007, *Science*, 315, 220. Reprinted with permission from AAAS.

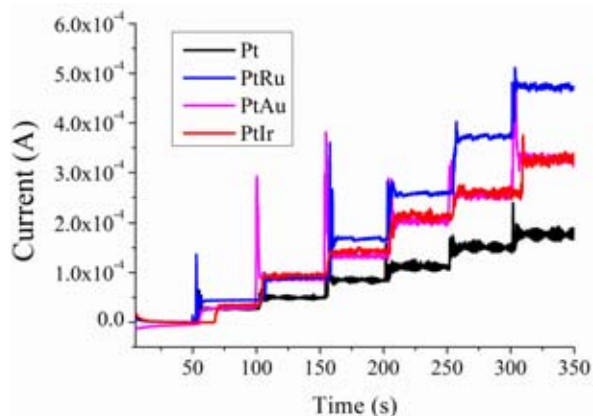


Fig. 14. Typical amperometric response of various catalysts in different concentrations of H_2O_2 (0.25 mM, 0.5 mM, 0.75 mM, 1.25 mM, 2.25 mM, 3.25 mM) [55].

enhanced catalytic activity towards glucose electro-oxidation. The improvement of Pt-Au may be attributed to the amount of surface Pt(0), the possible synergism between Pt and Au, the

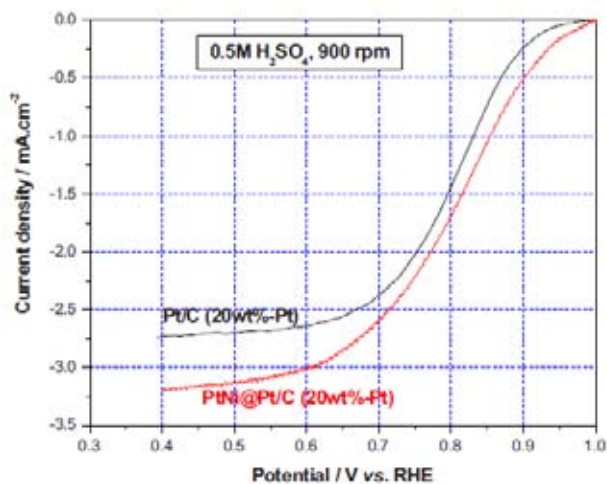


Fig. 15. Polarization curves for the ORR on Pt/C and PtNi@Pt/C catalysts by RDE in 0.5 M H_2SO_4 . Sweep rate: 5 mV/s, anodic sweep, room temperature. Reproduced from Li, W. and Haldar, P. 2010, *Electrochem. Solid State Lett.*, 13, B47, by permission of The Electrochemical Society.

surface modification provided by the presence of oxide/hydroxide species, and size effects [80]. Upadhyay *et al.* [81] found that the Au–PtNPs/3-APTES/GC modified electrode exhibited synergistic effects to increase the surface area, promote the ability to enhance electron transfer and good electrocatalytic activity for H₂O₂, and provide a new electrochemical platform for rapid detection with a high sensitivity in the presence of inhibitors. Zhang *et al.* [55] reported that the electrocatalytic properties of bimetals such as PtRu and PtAu catalysts show better performance in both sensitivity and selectivity than the pure Pt at a low applied potential, thus providing an anti-interference catalyst platform for future biological applications. For comparison, the sensitivities of PtRu, and PtAu are estimated to be 539.01, and 415.46 $\mu\text{A mM}^{-1} \text{cm}^{-2}$, respectively, twice as high as that of the pure Pt (221.77 $\mu\text{A mM}^{-1} \text{cm}^{-2}$). Fig. 14 shows i-t curves for different metals in different concentrations of H₂O₂. By multiple addition of H₂O₂ with increasing time, the increment of current density was observed. It was found that the current density for pure Pt is much lower than that of bimetallic PtRu, PtAu and PtIr nanoparticles, especially as observed in high H₂O₂ concentration [55].

Xiao *et al.* [82] showed that PtAu alloy nanoparticles also display high electrocatalytic activity towards the reduction of H₂O₂. This reflects a remarkable synergistic effect for PtAu alloy nanoparticles in alkaline media, the presence of Au can reduce the strength of Pt-OH formation and provide needed adsorption sites for –OH species. In the chemisorption of the reaction intermediate from H₂O_{2ad} dissociation at Pt via forming HO₂^{–ad}, the species should have sufficient binding strength with Au in a further 2e[–] reduction to O₂. Wang *et al.* [83] similarly reported that the nanocomposite film (Au-PtNPs/nanoPAN/CS) exhibited a variety of good electrochemical characteristics including high sensitivity and good long-term stability. Because Au-PtNPs have unique catalytic properties and good biocompatibility, and Au-PtNPs and nanoPAN have synergistic augmentation for facilitating electron-transfer. On the other hand, Lee *et al.* [84] have shown that macroporous Au-Pt exhibited an extremely high sensitivity of 264 mA mM^{–1} cm^{–2} in the concentration range up

to ~10 mM, in comparison to that of macroporous Au electrodes that show a sensitivity of 110 mA mM^{–1} cm^{–2}. The electro-catalytic activity toward the oxidation of H₂O₂ could be most likely caused by the enlarged surface activation area or surface roughness factor, which might provide many favorable sites for electron transfer.

Over the past years, a broad range of binary materials were used to design biosensors and fuel cells, providing new catalytic properties with minimal applied potential required and better selectivity than corresponding single metal materials. Ultimately, the advantage of the bimetallic catalyst approach by reducing the amount of precious metals can become a solution for economic impact by bringing up potential practical manufacturing processes without compromising their performance.

C. Platinum nickel catalysts (Pt-Ni)

The Pt-Ni alloy catalysts were widely used as fuel cell catalysts for MOR and ORR. According to literatures, both the bi-functional and electronic effects were ascribed to explain the enhancement of electrocatalytic activity of bimetallic catalysts for MOR and ORR. For the electronic effect, the electronic properties of bimetallic catalysts were altered by adding additional elements and further enlarging the active surface sites. For the bi-functional effect, by combining different materials each with its own unique catalytic properties, the synergetic effect was observed to produce more active catalytic surfaces [73, 85, 86]. Accordingly, the electronic structure of Pt could be changed by alloying with Ni. For example, Jiang *et al.* [87] have reported that based on DFT calculations, the charge transfer from Ni to Pt in Pt_mNi_n clusters formed a weakened CO adsorption on Pt_mNi_n clusters. Furthermore, Wenzhen Lia and co-workers, [88] who synthesized carbon supported core-shell PtNi@Pt nanoparticle catalysts through a two-step solution-phase reduction method, demonstrated a higher specific activity (SA) to ORR compared to a conventional Pt/C. This effect was attributed to the modified electronic structure of the Pt surface layer. Figure 15 shows the ORR data on Pt/C and PtNi@Pt/C catalysts obtained with an RDE in 0.5 M H₂SO₄ solution.

The core-shell PtNi@Pt/C catalysts exhibit a 5.4 times higher ORR activity than commercial Pt/C [88].

Kim *et al.* [89] have demonstrated that the Pt-Ni alloy catalyst heat-treated at 400°C showed the best activity in methanol oxidation due to the change in Pt electronic structure by Ni and had a lower energy shift in the binding energy of Pt 4f electrons, as characterized by X-ray photoelectron spectroscopy (XPS). On the other hand, the bi-functional mechanism is also widely discussed to be an important issue for designing highly electrocatalytic activity of Pt-based catalysts. Zhou *et al.* [90] showed that the PtNi hollow nanospheres exhibited better performance than Pt/C catalysts for MOR which can be explained by the bi-functional mechanism, the Pt electronic structure change and its especial hollow structure. Moreover, Deivaraj *et al.* [91] also proposed similar results with respect to promotion of MOR performance by the bi-functional mechanism. According to CV results in the work of Liu *et al.* [92], a linear relationship was found between the peak current densities and the number of Pt-Ni interfaces for the multisegment PtNi nanorods. The increase in catalytic activity with the number of Ni/Pt interfaces can also be seen, thus providing a direct demonstration of the role of active pair sites in the bi-functional mechanism.

D. Platinum-other metals

Aside from the bimetallic materials discussed above, there are many other Pt-based bimetallic materials employed to improve the catalytic performance and decrease the interference of co-existent species such as Ascorbic Acid (AA). With onion-like mesoporous carbon vesicles as a template, the PtPd bimetallic alloy nanoparticles were prepared by a facile and fast microwave irradiation method [93]. Compared with the Pt catalysts, the PtPd bimetallic catalysts electrode displayed enhanced current response towards glucose in the linear range from 1.5 to 12 mM, and achieved 95% of the steady-current within 3s. In addition, the influence of Pt/Pd weight ratios on the electrocatalytic activity of PtPd towards glucose oxidation was also investigated. Fig. 16 compares the effect of different Pt/Pd weight ratios on the response for 50 mM glucose in 0.1 M phosphate buffered saline (PBS). The Pt(25)

Pd(25) catalyst gave the highest amperometric response in comparison with other weight ratios. This non-enzymatic glucose sensor also exhibited good ability of anti-interference to AA, uric acid, and dopamine (shown in Fig. 16).

These Pt-based nanomaterials can be combined with functionalized membranes to form hybrid materials, which could be used for wider range of electroanalytical applications. The combination of the electrocatalytic activities of bimetallic nanomaterials and the stability or conductivity of membranes is desirable for biosensor fabrication. For instance, highly dispersed PtM (M= Ru, Pd and Au) nanoparticles on composite films of multi-walled carbon nanotubes (MWNTs) in ionic liquids demonstrated stronger electrocatalytic activities for glucose [94]. By comparing the voltammetric behavior of single Pt and bimetallic nanocatalysts, it was found that the area of hydrogen adsorption/desorption peak increased after alloying with the second metal. The second metal is a crucial factor affecting the electrochemical activity of bimetallic nanocatalysts. The nano-composite modified with MWNTs and ionic liquid also demonstrated smaller electron transfer resistance and larger active surface area than pure bimetallic nanoparticles. Even at low applied potential (-0.1V), the electrode responded linearly to glucose up to 15 mM, with a detection limit of 0.05 mM (S/N = 3) and detection sensitivity of 10.7 $\mu\text{Acm}^{-2}\text{mM}^{-1}$. Meanwhile, the interference of AA, uric acid, acetamidophenol and fructose were effectively avoided.

It has been demonstrated that surface strain is correlated with catalytic activities of metals [21, 95]. Nanoporous PtAg and PtCu alloys were obtained by a simple galvanic replacement of nanoporous silver and copper with H_2PtCl_6 [96]. After incorporation into glucose sensors, the higher electrocatalytic activity of nanoporous PtAg was observed compared with that of nanoporous PtCu (shown in Fig. 17). The larger lattice parameter of Ag resulted in a larger tensile strain in the PtAg alloy, which may explain higher electrocatalytic activity of nanoporous PtAg than nanoporous PtCu.

Adsorbed carbon monoxide (CO) on Pt has been widely accepted as the main poisoning species in various electrocatalytic reactions. In the case of

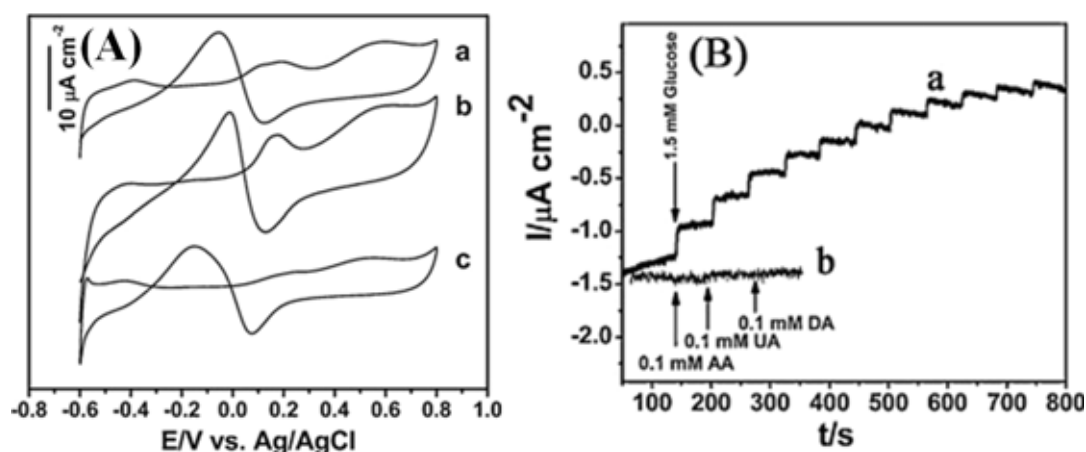


Fig. 16. (A) CV curves of PtPd bimetallic catalysts with different atomic ratios (a: Pt(66)Pd(34); b: Pt(50)Pd(50) c: Pt(34)Pd(66)). (B) The amperometric $i-t$ curve of Pt(50)Pd(50) electrode with successive additions of 1.5 mM glucose at +0.55 V. Reprinted from Bo, X. *et al.*, *Sens. Actuator B-Chem.*, 157, 662, Copyright (2011) with permission from Elsevier.

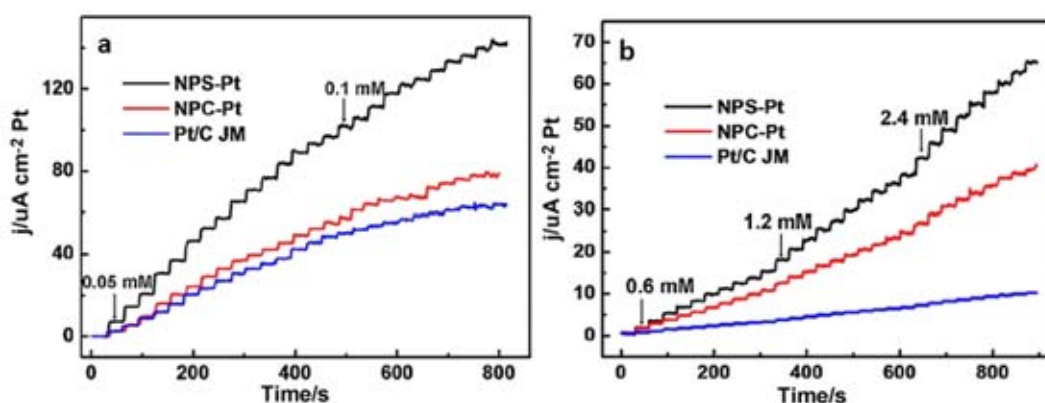
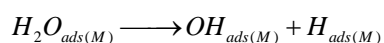


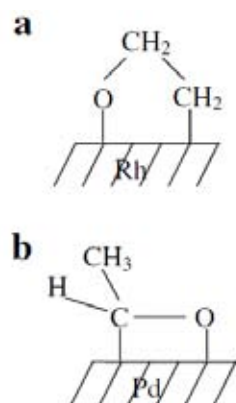
Fig. 17. Amperometric current responses of $\text{GO}_x/\text{NPS-Pt}$ (nanoporous silver-platinum), $\text{GO}_x/\text{NPC-Pt}$ (nanoporous copper-platinum), $\text{GO}_x/\text{Pt/C}$ modified GCEs on successive addition of H_2O_2 (a) and glucose (b) into stirring PBS (0.1 M, pH 7.0). Reprinted from Xu, C. *et al.*, *Biosens. Bioelectron.*, 27, 160, Copyright (2011) with permission from Elsevier.

DMFCs, methanol with large amount of water is utilized at the anode. If there is a second metal, which could easily dehydrogenate the molecular H_2O , then the oxidation of CO to CO_2 will be efficient. With binary catalysts in the DMFC, the promotion effect of a second metal (M) in Pt–M is attributed to the bi-functional mechanism [97]. On a pure Pt, $\text{H}_2\text{O}_{\text{ads(Pt)}}$ dissociation is difficult [98] and relatively high positive electrode potential is needed to “activate” H_2O molecules. Pt sites serve to adsorb and dehydrogenate methanol, and M provide nucleation sites for OH_{ads} formation.

The reaction between $\text{CO}_{\text{ads(Pt)}}$ and $\text{OH}_{\text{ads(M)}}$ facilitates oxidation by removing the carbon monoxide.



Recently, from a relativistic density-functional study of CO adsorption, analysis of the energetics of H_2O dissociation, and the reaction between CO_{ads} and OH_{ads} has been carried out on a series of Pt–M mixed metal clusters [99].



Scheme 1. An oxametallacyclic conformation formed during ethanol adsorbed on an Rh (111) surface (a) and n²-acetaldehyde formed during ethanol adsorbed on a Pd (111) surface (b). Reprinted from Shen, S. Y. *et al.*, *Int. J. Hydrog. Energy*, 35, 12911, Copyright (2010) with permission from Elsevier.

Table 1. Differential electrochemical mass spectrometry (DEMS) signal ratios of the ($m/z = 44$)/($m/z = 29$) for the different electrode compositions. Reprinted with permission from De Souza, J. P. I. *et al.*, *J. Phys. Chem. B*, 106, 9825. Copyright (2002) American Chemical Society.

electrode	($m/z = 44$)/($m/z = 29$) $E = 0.7$ V
Pt	0.17
Pt ₉₀ Rh ₁₀	0.17
Pt ₇₃ Rh ₂₇	0.49
Pt ₅₅ Rh ₄₅	0.67
Rh	1.8

The $\text{CO}_{\text{ads(Pt)}}$ adsorption energies on Pt, Pt-C and C-O bond lengths, force constants, stretching frequencies in mixed Pt-M surfaces were calculated. On the basis of the calculated adsorption energies of H₂O, OH, and H, the reaction energies and activation barriers for H₂O_{ads(M)}} dissociation on the M site were estimated. For most of the mixed Pt-M metal surfaces, the presence of M weakened the Pt-C bond and lowered the C-O stretching frequency. The $\text{CO}_{\text{ads(Pt)}}$ adsorption energy was decreased dramatically by the presence of second metals. These metals also showed much higher activity as bi-functional catalysts toward H₂O_{ads(M)}} dissociation and formation of OH_{ads(M)}} than pure Pt.

The other reason for sluggish reactivity in fuel cells is the inefficient C-C bond cleavage. Many researchers have suggested that addition of Rh increases the ability for C-C bond dissociation and thereby improved the selectivity towards CO₂ production compared to pure Pt [100]. Owing to the formation of an oxametallacyclic conformation (shown in Scheme 1a), the C-C bond cleavage is the preferential channel for the ethanol dissociation on the Rh surface [101], while n²-acetaldehyde (Scheme 1b) is preferred on Pt or Pd surfaces [102]. In this study the addition of Rh to Pt can increase the CO₂ yield during the ethanol oxidation [103].

The electrochemical oxidation of ethanol on Pt, Rh, and Pt-Rh electrodes has been studied by using on-line differential electrochemical mass spectrometry (DEMS) and *in-situ* infrared spectroscopy (FTIR) [104]. Acetaldehyde was determined by the mass signal $m/z = 29$ corresponding to the fragment [CHO]⁺. The mass signal for $m/z = 44$ was the main peak of true CO₂ fragmentation, corresponding to [CO₂]⁺. The results were normalized using the oxidation of a CO monolayer in order to compare the activity of the different electrodes. The ratios of CO₂/CH₃CH₂O increases when Rh is added to the electrode (shown in Table 1). The possible reasons for the different reactivity for the studied electrodes were discussed in terms of C-H bond activation and C-O bond coupling on the different surfaces. A study on the temperature-dependence of the electrocatalytic activities afforded the determination of apparent activation energies for ethanol oxidation [105]. A pronounced effect of catalyst composition on ethanol oxidation was observed. The results also indicated that the enhancement in electrocatalytic activity for PtRh catalyst in comparison to Pt itself can be ascribed to an improvement of C-C bond dissociation rather than to a bi-functional mechanism. Here, both the structural modification via lattice parameter change and the electronic modification through charge transfer from metal to metal could kinetically facilitate the sluggish electrode reaction with an increased electrocatalytic performance [106].

V. SUMMARY AND OUTLOOK

Bimetallic catalysts have demonstrated great potential in the area of energy and biosensing

applications. Bimetallic nanosystems have been shown to exhibit an enhancement in specific properties upon alloying. In hydrogen fuel cells, pure Pt anode electrocatalysts are severely poisoned by trace amounts of carbon monoxide that are ubiquitous in H₂ fuels. Therefore, bimetallic Pt-M electrocatalysts (M = Ru, Mo, Sn, Rh) have been employed due to their higher CO tolerance, which leads to more efficient catalysts compared to pure Pt nanoparticles.

Bimetallic nanoparticles maybe tuned not only by varying the size of the nanostructure but by changing the composition and chemical ordering pattern as well. To date the most popular bimetallic nano alloys are formed from mixing the transition metal elements, giving rise to a large group of 276 possible binary combinations. Furthermore, the degree of mixing and chemical ordering in bimetallic alloys can be varied, and diverse chemical ordering patterns can be designed for nanoalloys. To reach the full potential of bimetallic catalysts in practical applications, a fundamental understanding on the particle size, composition and chemical ordering pattern affecting the electrochemical properties will be needed. Therefore, the development of new alloy structures and the systematic study of their properties are required.

ACKNOWLEDGEMENT

The preparation of this manuscript and research in our laboratory are supported by the NSF grant #100768, Delta Environmental & Educational Foundation (DEEF), Taiwan, Royal Thai Government Fellowship, Taiwan National Central University Fellowship, and China Scholarship Council Postgraduate Scholarship Program.

REFERENCES

1. Wang, F. and Hu, S. 2009, *Microchim. Acta.*, 165, 1.
2. Rahman, M. A., Noh, H. B., and Shim, Y. B. 2008, *Anal. Chem.*, 80, 8020.
3. Tang, B., Cao, L., Xu, K., Zhuo, L., Ge, J., Li, Q., and Yu, L. 2008, *Chem. Eur. J.*, 14, 3637.
4. Fang, L., Li, W., Zhou, Y., and Liu, C. C. 2009, *Sens. Actuator B-Chem.*, 137, 235.
5. Lersch, M. and Tilset, M. 2005, *Chem. Rev.*, 105, 2471.
6. Sakamoto, Y., Okumura, K., Kizaki, Y., Matsunaga, S., Takahashi, N., and Shinjoh, H. 2006, *J. Catal.*, 238, 361.
7. Wu, H., Wang, J., Kang, X. H., Wang, C. M., Wang, D. H., Liu, J., Aksay, I. A., and Lin, Y. H. 2009, *Talanta*, 80, 403.
8. Zou, Y. J., Xiang, C. L., Sun, L. X., and Xu, F. 2008, *Biosens. Bioelectron.*, 23, 1010.
9. Wang, Z. L., Ahmad T. S., and ElSayed, M. A. 1997, *Surf. Sci.*, 380, 302.
10. Zhigang, S., Baolian, Y., and Ming, H. 1999, *J. Power Sources*, 79, 82.
11. Hall, S. B., Khudaish, E. A., and Hart, A. L. 2000, *Electrochim. Acta*, 45, 3573.
12. Susut, C., Nguyen, T. D., Chapman, G. B., and Tong, Y. 2008, *Electrochim. Acta*, 53, 6135.
13. Carrette, L., Friedrich, K. A., and Stimming, U. 2000, *Chemphyschem*, 1, 162.
14. Ghenciu, A. F. 2002, *Curr. Opin. Solid State Mat. Sci.*, 6, 389.
15. Hamnett, A. 1997, *Catal. Today*, 38, 445.
16. Gasteiger, H. A., Kocha, S. S., Sompalli, B., and Wagner, F. T. 2005, *Appl. Catal. B-Environ.*, 56, 9.
17. Norskov, J. K., Rossmeisl, J., Logadottir, A., Lindqvist, L., Kitchin, J. R., Bligaard, T., and Jonsson, H. 2004, *J. Phys. Chem. B*, 108, 17886.
18. Mallat, T. and Baiker, A. 1994, *Catal. Today*, 19, 247.
19. Hammer, B., Norskov, J. K., Bruce, C., and Gates, H. K. 2000, *Adv. Catal.*, Academic Press, 71.
20. Greeley, J., Stephens, I. E. L., Bondarenko, A. S., Johansson, T. P., Hansen, H. A., Jaramillo, T. F., Rossmeisl, J., Chorkendorff, I., and Nørskov, J. K. 2009, *Nat. Chem.*, 1, 552.
21. Stamenkovic, V., Mun, B. S., Mayrhofer, K. J. J., Ross, P. N., Markovic, N. M., Rossmeisl, J., Greeley, J., and Nørskov, J. K. 2006, *Angew. Chem. Int. Edit.*, 45, 2897.
22. Adams, W. A., Blair, J., Bullock, K. R., and Gardner, C. L. 2005, *J. Power Sources*, 145, 55.
23. Papageorgopoulos, D. C. and de Bruijn, F. A. 2002, *J. Electrochem. Soc.*, 149, A140.
24. Watanabe, M. and Motoo, S. 1975, *J. Electroanal. Chem.*, 60, 275.

25. Ianniello, R., Schmidt, V. M., Stimming, U., Stumper, J., and Wallau, A. 1994, *Electrochim. Acta*, 39, 1863.
26. Davies, J. C., Hayden, B. E., and Pegg, D. J. 1998, *Electrochim. Acta*, 44, 1181.
27. Ioroi, T., Yasuda, K., Siroma, Z., Fujiwara, N., and Miyazaki, Y. 2003, *J. Electrochem. Soc.*, 150, A1225.
28. Buatier de Mongeot, F., Scherer, M., Gleich, B., Kopatzki, E., and Behm, R. J. 1998, *Surf. Sci.*, 411, 249.
29. Iwasita, T., Hoster, H., John-Anacker, A., Lin, W. F., and Vielstich, W. 1999, *Langmuir*, 16, 522.
30. Gómez de la Fuente, J. L., Martínez-Huerta, M. V., Rojas, S., Terreros, P., Fierro, J. L. G., and Peña, M. A. 2006, *Catal. Today*, 116, 422.
31. Zhu, J., Su, Y., Cheng, F., and Chen, J. 2007, *J. Power Sources*, 166, 331.
32. Markovic, N. M., Gasteiger, H. A., Ross Jr, P. N., Jiang, X., Villegas, I., and Weaver, M. J. 1995, *Electrochim. Acta.*, 40, 91.
33. Dao-Jun, G. 2010, *J. Power Sources*, 195, 7234.
34. Seiler, T., Savinova, E. R., Friedrich, K. A., and Stimming, U. 2004, *Electrochim. Acta.*, 49, 3927.
35. Guo, J., Sun, G., Shiguo, S., Shiyu, Y., Weiqian, Y., Jing, Q., Yushan, Y., and Qin, X. 2007, *J. Power Sources*, 168, 299.
36. Seo, S. H. and Lee, C. S. 2010, *Appl. Energy*, 87, 2597.
37. Scott, K., Taama, W. M., Argyropoulos, P., and Sundmacher, K. 1999, *J. Power Sources*, 83, 204.
38. Du, C. Y., Zhao, T. S., and Yang, W. W. 2007, *Electrochim. Acta*, 52, 5266.
39. Park, H., Kim, Y., Choi, Y. S., Hong, W. H., and Jung, D. 2008, *J. Power Sources*, 178, 610.
40. Alayoglu, S., Nilekar, A. U., Mavrikakis, M., and Eichhorn, B. 2008, *Nat. Mater.*, 7, 333.
41. Campbell, C. T. 1990, *Annu. Rev. Phys. Chem.*, 41, 775.
42. Rodriguez, J. A. and Goodman, D. W. 1992, *Science*, 257, 897.
43. Park, K. W., Ahn, K. S., Choi, J. H., Nah, Y. C., and Sung, Y. E. 2003, *Appl. Phys. Lett.*, 82, 1090.
44. Umeda, M., Ojima, H., Mohamedi, M., and Uchida, I. 2004, *J. Power Sources*, 136, 10.
45. Wang, Z. B., Zuo, P. J., and Yin, G. P. 2009, *J. Alloy. Compd.*, 479, 395.
46. Garcia, G., Tsiouvaras, N., Pastor, E., Pena, M. A., Fierro, J. L. G., and Martínez-Huerta, M. V. 2011, *Int. J. Hydrog. Energy*, in press.
47. Chen, S., Ye, F., and Lin, W. 2010, *Int. J. Hydrog. Energy*, 35, 8225.
48. Kang, D. K., Noh, C. S., Kim, N. H., Cho, S. H., Sohn, J. M., Kim, T. J., and Park, Y. K. 2010, *J. Ind. Eng. Chem.*, 16, 385.
49. Zhao, H., Li, L., Yang, J., and Zhang, Y. 2008, *Electrochem. Commun.*, 10, 1527.
50. Kim, J., Poliquit, B. Z., Nam, H. S., Kim, S. H., Lee, Y. M., Kim, K. M., and Ko, J. M. 2012, *Curr. Appl. Phys.*, 12, 254.
51. Yoo, J. S., Kim, H. T., Joh, H. I., Kim, H., and Moon, S. H. 2011, *Int. J. Hydrog. Energy*, 36, 1930.
52. Chu, Y. H. and Shul, Y. G. 2010, *Int. J. Hydrog. Energy*, 35, 11261.
53. Wang, Z. B., Yin, G. P., Zhang, J., Sun, Y. C., and Shi, P. F. 2006, *Electrochim. Acta*, 51, 5691.
54. Janyasupab, M., Zhang, Y., Lin, P. Y., Bartling, B., Xu, J., and Liu, C. C. 2011, *J. Nanotechnol.*, doi:10.1155/2011/506862
55. Zhang, Y., Janyasupab, M., Liu, C. W., Lin, P. Y., Wang, K. W., Xu, J., and Liu, C. C. 2012, *Int. J. Electrochem.*, in press.
56. Li, L. H., Zhang, W. D., and Ye, J. S. 2008, *Electroanalysis*, 20, 2212.
57. Liu J. and Wang, J. 2001, *Food Technol. Biotechnol.*, 39, 55.
58. Luo, J., Maye, M. M., Kariuki, N. N., Wang, L., Njoki, P., Lin, Y., Schadt, M., Naslund, H. R., and Zhong, C. J. 2005, *Catal. Today*, 99, 291.
59. Luo, J., Maye, M. M., Petkov, V., Kariuki, N. N., Wang, L., Njoki, P., Mott, D., Lin, D., and Zhong, C. J. 2005, *Chem. Mater.*, 17, 3086.
60. Maye, M. M., Kariuki, N. N., Luo, J., Han, J., Njoki, P., Wang, L., Lin, Y., Naslund, H. R., and Zhong, C. J. 2004, *Gold Bull.*, 37, 3.
61. Njoki, P. N., Luo, J., Wang, L., Maye, M. M., Quaizar, H., and Zhong, C. J. 2005, *Langmuir*, 21, 1623.

62. Zhong, C. J., Luo, J., Maye, M. M., Han, L., and Kariuki, N. N. 2004, *Nanotechnology in Catalysis*, Zhou, B., Hermans, S. and Somorjai, G. A. (Ed.), Kluwer Academic/Plenum: New York, 222.
63. Liu, C. W., Wei, Y. C., and Wang, K. W. 2009, *J. Colloid Interface Sci.*, 336, 654.
64. Antolini, E., Salgado, J. R. C., and Gonzalez, E. R. 2005, *J. Electroanal. Chem.*, 580, 145.
65. Salgado, J. R. C., Antolini, E., and Gonzalez, E. R. 2004, *J. Phys. Chem. B*, 108, 17767.
66. Salgado, J. R. C., Antolini, E., and Gonzalez, E. R. 2005, *Appl. Catal. B-Environ.*, 57, 283.
67. Hernandez-Fernandez, P., Rojas, S., Ocon, P., de Frutos, A., Figueroa, J. M., Terreros, P., Pena, M. A., and Fierro, J. L. G. 2008, *J. Power Sources*, 177, 9.
68. Wang, J., Yin, G., Wang, G., Wang, Z., and Gao, Y. 2008, *Electrochem. Commun.*, 10, 831
69. Choi, J. H., Park, K.W., Park, I. S., Kim, K., Lee, J. S., and Sung, Y. E. 2006, *J. Electrochem. Soc.*, 153, A1812.
70. Song, C., Ge, Q., and Wang, L. 2005, *J. Phys. Chem. B*, 109, 22341.
71. Du, B. and Tong, Y. Y. 2005, *J. Phys. Chem. B*, 109, 17775.
72. Luo, J., Njoki, P. N., Lin, Y., Wang, L., and Zhong, C. J. 2006, *Electrochem. Commun.*, 8, 581.
73. Stamenkovic, V. R., Mun, B. S., Arenz, M., Mayrhofer, K. J. J., Lucas, C. A., Wang, G., Ross, P. N., and Markovic, N. M. 2007, *Nat. Mater.*, 6, 241.
74. Hernandez-Fernandez, P., Rojas, S., Ocon, P., Gomez de la Fuente, J. L., San Fabian, J., Sanza, J., Pena, M. A., Garcia-Garcia, F. J., Terreros, P., and Fierro, J. L. G. 2007, *J. Phys. Chem. C*, 111, 2913.
75. Liu, C. W., Wei, Y. C., and Wang, K. W. 2009, *Electrochem. Commun.*, 11, 1362.
76. Bus, E. and Van Bokhoven, J. A. 2007, *J. Phys. Chem. C*, 111, 9761.
77. Zhang, J., Vukmirovic, M. B., Xu, Y., Mavrikakis, M., and Adzic, R. R. 2005, *Angew. Chem. Int. Edit.*, 44, 2132.
78. Nilekar, A. U. and Mavrikakis, M. 2008, *Surf. Sci.*, 602, L89.
79. Zhang, J., Sasaki, K., Sutter, E., and Adzic, R. R. 2007, *Science*, 315, 220.
80. Singh, B., Laffir, F., McCormac, T., and Dempsey, E. 2010, *Sens. Actuator B-Chem.*, 150, 80.
81. Upadhyay, S., Rao, G. R., Sharma, M. K., Bhattacharya, B. K., Rao, V. K., and Vijayaraghavan, R. 2009, *Biosens. Bioelectron.*, 25, 832.
82. Xiao, F., Zhao, F., Zhang, Y., Guo, G., and Zeng, B. 2009, *J. Phys. Chem. C*, 113, 849.
83. Wang, X., Yang, T., Feng, Y., Jiao, K., and Li, G. 2009, *Electroanalysis*, 21, 819
84. Lee, Y. J., Park, J. Y., Kim, Y., and Ko, J. W. 2011, *Curr. Appl. Phys.*, 11, 211.
85. Mukerjee, S. 1990, *J. Appl. Electrochem.*, 20, 537.
86. Murthi, V. S., Urian, R. C., and Mukerjee, S. 2004, *J. Phys. Chem. B*, 108, 11011.
87. Jiang, Q., Jiang, L., Hou, H., Qi, J., Wang, S., and Sun, G. 2010, *J. Phys. Chem. C*, 114, 19714.
88. Li, W. and Haldar, P. 2010, *Electrochem. Solid State Lett.*, 13, B47.
89. Kim, D. B., Chun, H. J., Lee, Y. K., Kwon, H. H., and Lee, H. I. 2010, *Int. J. Hydrog. Energy*, 35, 313.
90. Zhou, X. W., Zhang, R. H., Zhou, Z. Y., and Sun, S. G. 2011, *J. Power Sources*, 196, 5844.
91. Deivaraj, T. C., Chen, W., and Lee, J. Y. 2003, *J. Mater. Chem.*, 13, 2555.
92. Liu, F., Lee, J. Y., and Zhou, W. 2004, *J. Phys. Chem. B*, 108, 17959.
93. Bo, X., Bai, J., Yang, L., and Guo, L. 2011, *Sens. Actuator B-Chem.*, 157, 662.
94. Xiao, F., Zhao, F., Mei, D., Mo, Z., and Zeng, B. 2009, *Biosens. Bioelectron.*, 24, 3481.
95. Mavrikakis, M., Hammer, B., and Norskov, J. K. 1998, *Phys. Rev. Lett.*, 81, 2819.
96. Xu, C., Liu, Y., Su, F., Liu, A., and Qiu, H. 2011, *Biosens. Bioelectron.*, 27, 160.
97. Watanabe, M., Uchida, M., and Motoo, S. 1987, *J. Electroanal. Chem.*, 229, 395.
98. Ishikawa, Y., Liao, M. S., and Cabrera, C. R. 2000, *Surf. Sci.*, 463, 66.
99. Ishikawa, Y., Liao, M. S., and Cabrera, C. R. 2002, *Surf. Sci.*, 513, 98.

-
100. Kowal, A., Li, M., Shao, M., Sasaki, K., Vukmirovic, M. B., Zhang, J., Marinkovic, N. S., Liu, P., Frenkel, A. I., and Adzic, R. R. 2009, *Nat. Mater.*, 8, 325.
 101. Vesselli, E., Baraldi, A. Comelli, G. Lizzit, S., and Rosei, R. 2004, *Chemphyschem*, 5, 1133.
 102. Mavrikakis, M., Doren, D. J., and Barteau, M. A. 1998, *J. Phys. Chem. B*, 102, 394.
 103. Shen, S. Y., Zhao, T. S., and Xu, J. B. 2010, *Int. J. Hydrog. Energy*, 35, 12911.
 104. De Souza, J. P. I., Queiroz, S. L., Bergamaski, K., Gonzalez, E. R., and Nart, F. C. 2002, *J. Phys. Chem. B*, 106, 9825.
 105. Sen Gupta, S. and Datta, J. 2006, *J. Electroanal. Chem.*, 594, 65.
 106. Ren, H-X., Huang, X-J., Kim, J-H., Choi, Y-K., and Gu, N. 2009, *Talanta*, 78, 1371.